Enhanced CO_2 affinity in a metal-organic framework through green incorporation of a dual-functional amino acid

Edward Loukopoulos,*[a] Sofía Barragán-Soto[a], Sergio Marugán-Benito[a], Emilio Borrego-Marín,[b] Jorge A. R. Navarro[b] and Ana E. Platero-Prats*[a,c]

[a] Departamento de Química Inorgánica, Facultad de Ciencias, Universidad Autónoma de Madrid, Campus de Cantoblanco, 28049 Madrid, Spain

[b] Departamento de Química Inorgánica, Universidad de Granada, 18071 Granada, Spain

[b] Condensed Matter Physics Center (IFIMAC), Universidad Autónoma de Madrid, 28049, Campus de Cantoblanco, 28049 Madrid, Spain

SUPPORTING INFORMATION

Table of contents	Page

Supplementary Methods

Materials. All reagents were used as received from commercial suppliers without further purification. Certain batches of the pristine DUT-67 material were also used in another recent study of our group[1] and therefore share the same characterization (TGA, SEM) results.

NMR spectroscopy: ^{1}H-NMR spectra were acquired on a Bruker Avance NEO-500 spectrometer, running at 500MHz. MOF samples were prepared by digesting a small portion (~5 mg) of each solid in a DMSO-d_6 (500 μL) / D_2O (100 μL) / HF (25 μL) solution. Chemical shifts (δ) are reported in parts per million (ppm) relative to the residual solvent signal with a value of 2.50 ppm for DMSO-d_6.

Powder X-Ray Diffraction (PXRD): PXRD patterns were collected using a Bruker D8 diffractometer equipped with a copper source operating at 1600 W. The samples were ground and placed onto a borosilicate sample holder, and the surface was levelled with a clean microscope slide. The diffraction patterns were collected in continuous mode over a 2θ range of 3 to 45 degrees, with a step size of 0.02° and an exposure time of 0.5 s per step. Calculated PXRD patterns from the corresponding single-crystal data were obtained using Mercury 3.8.[2]

Scanning Electron Microscope (SEM): Images were obtained using a JEOL JSM 7600 F microscope.

Fourier-transform infrared (FT-IR) spectroscopy: Spectra were recorded on a PerkinElmer 100 spectrophotometer using a PIKE Technologies MIRacle Single Reflection Horizontal ATR Accessory from 4000–450 cm^{-1}.

Gas sorption studies: Low pressure gas sorption measurements were carried out at various temperatures (77 K for N_2, 273 and 298 K for CO_2) using a Micromeritics 3Flex Surface and Catalyst Characterization Analyzer system. Prior to analysis, the samples were activated under dynamic vacuum at 100 °C for 15 hours to remove all solvent molecules from the pores. Activation was performed on the degasser port of the instrument using a specific amount of MOF inside a 12 mm sample cell tube. The cell was then transferred to the analysis port of the instrument. After the measurement, the sample was re-weighed to obtain its precise mass and perform data analysis.

Pore-size-distribution (PSD) curves were obtained from the adsorption branches using non-local density functional theory (NLDFT) method for a cylinder pore in pillared clays. To regenerate the samples after a CO_2 sorption, the samples were subjected to dynamic vacuum (0.5 Torr) at 100 ºC for 90 minutes.

To calculate the isosteric heat of adsorption (ΔH_{ads}), isotherm data were first fitted using the Freundlich–Langmuir equation:

$$n = \frac{a \cdot b \cdot p^c}{a + b \cdot p^c}$$

Where n = the amount adsorbed (mmol g^{-1}) p = pressure (kPa), a = maximum loading (mmol g^{-1}), b = affinity constant (1/kPa^c) and c = heterogeneity exponent.

ΔH_{ads} was then calculated as reported elsewhere[3] using the Clausius-Clapeyron equation:

$$-\Delta H_{ads}(n) = -R \cdot ln\frac{p_2}{p_1}\frac{T_1 \cdot T_2}{(T_2 - T_1)}$$

Where p = pressure, T = temperature, R = ideal gas constant.

Thermogravimetric Analysis (TGA): Measurements were performed using an SDT Q600 from TA Instruments equipment in a temperature range between 20 °C and 800 °C under air (100 mL min^{-1} flow) atmosphere and heating rate of 10 °C·min^{-1}.

Supplementary Note 1. Synthesis and Characterization of pristine MOFs

Synthesis of pristine DUT-67: $ZrCl_4$ (460 mg, 2 mmol) was added to a 100 mL glass bottle along with 50 mL of a DMF/NMP mixture (1:1), followed by ultrasonication for 2 min to dissolve the solid. H_2TDC (220 mg, 1.34 mmol) was then added, and the mixture was further sonicated for 2 min. HCOOH (8.9 mL) was then added and the resulting mixture was placed in an oven for 48 h at 130 °C. A white crystalline solid was formed during this period. After allowing the mixture to cool to room temperature, the solid material was washed with DMF, ethanol (5 times each) and methanol (2 times) and dried in an oven at 60 °C. Yield: 379 mg. ^{1}H-NMR (Figure S3): δ 8.10 (s, 2H, 2 × HCOO), 7.71 (s, 8H, 4 x TDC). Other peaks: 7.90 (s, 0.5 H, DMF), 3.43 (q, *J*=7.0 Hz, 3H,

EtOH), 3.15 (s, MeOH), 2.87 (s, 2H, DMF), 2.71 (s, 2H, DMF), 1.04 (t, *J*=7.0 Hz, 3H, EtOH). Chemical Formula: $[Zr_6O_6(OH)_2(TDC)_4(HCOO)_2(solvent)_4]$

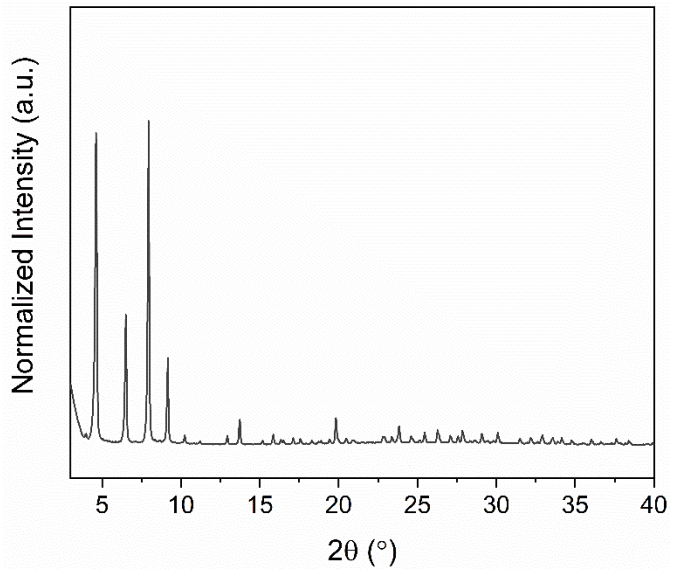

Figure S1. PXRD pattern of pristine DUT-67.

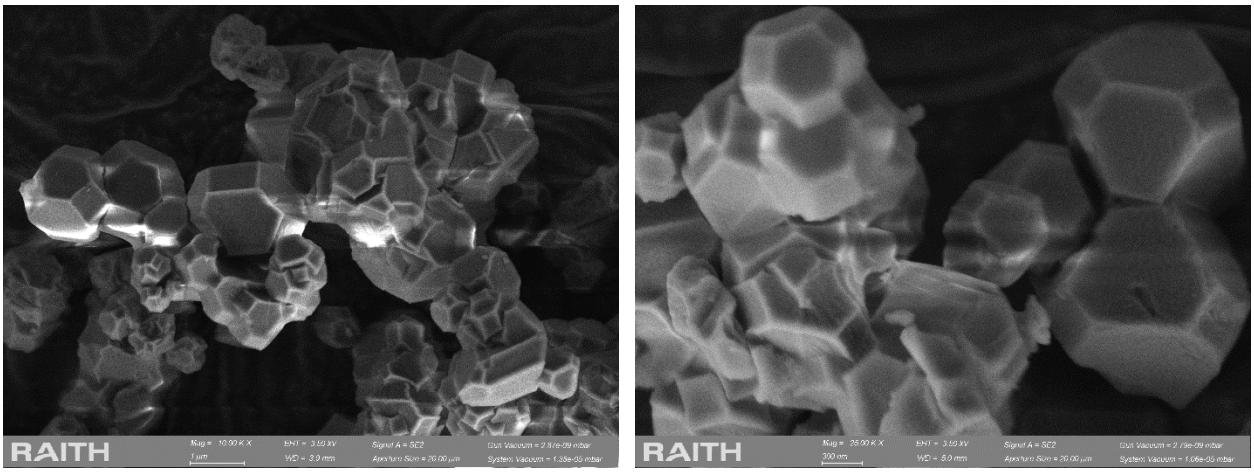

Figure S2. SEM images of pristine DUT-67. The material is highly crystalline and the particles display a truncated octahedron morphology that resembles a truncated octahedron (edge size ranging from 0.5 to 1 μm) as per previous reports.[1,4]

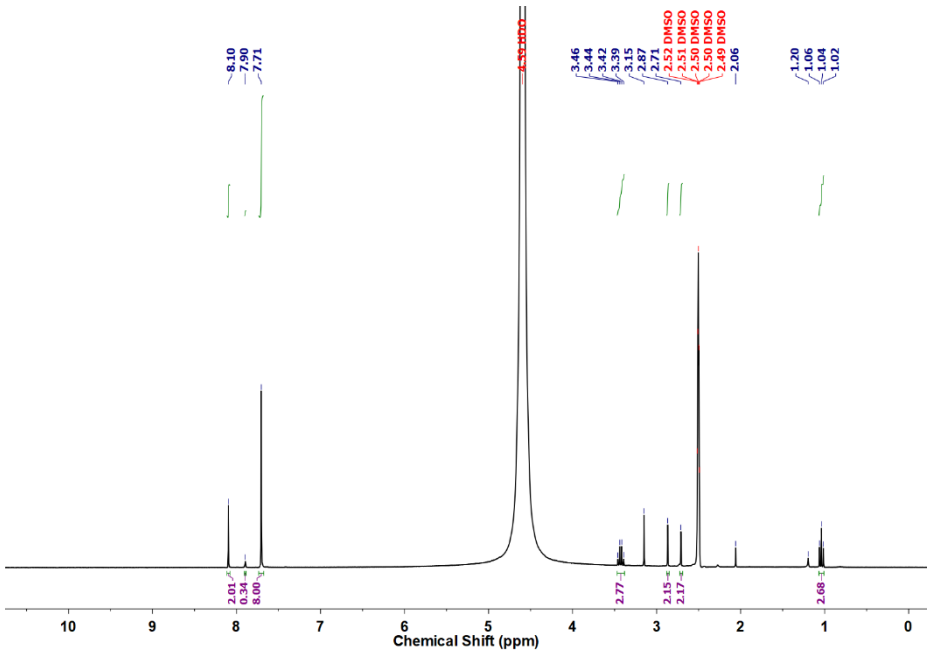

Figure S3. ^{1}H-NMR of pristine DUT-67 in DMSO-d_6:D_2O:HF (500 MHz).

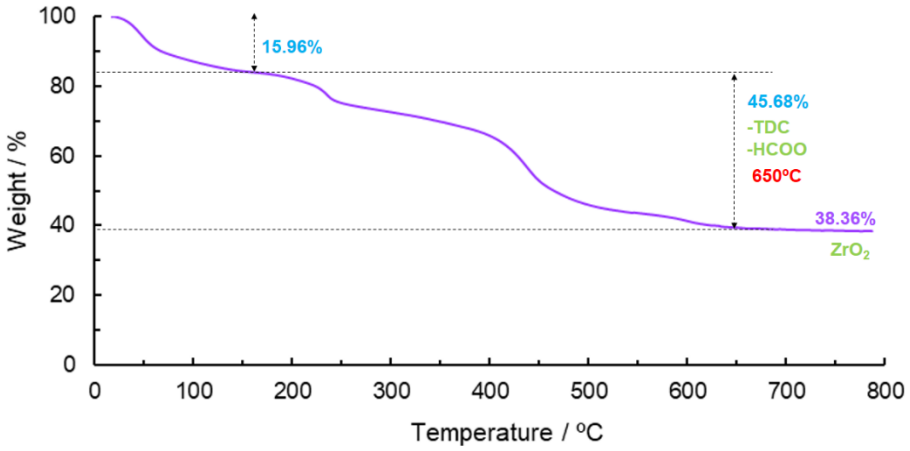

Figure S4. TGA of pristine DUT-67. Initial loss at 100-130 °C corresponds to solvent molecule removal. The main framework remains stable up to approximately ~200 °C, where the organic component (main linker and formates) begin to decompose leaving only ZrO_2 as the final residue by 600 °C (calcd. loss: 49.1%, exper. loss: 45.7%).

Supplementary Note 2. Synthesis and Characterization of functionalized MOFs

Synthesis of DUT-67-pro: 30 mg (0.02 mmol) of DUT-67 were added in a 20 ml glass capped vial containing L-proline (28 mg, 0.24 mmol) and 5 ml of EtOH. Four drops of HCl (37%) were then added to the solution. The resulting mixture was stirred at 80 ºC for 48 h. The white solid was washed with ethanol (5 times) and methanol (2 times), then dried at 60 ºC for 24 h. Yield: 34 mg. ^{1}H-NMR (Figure S5): δ 8.07 (s, 0.7H, HCOO), 7.69 (s, 8H, 4 x TDC), 4.23 (t, *J* = 7.8 Hz, 4H, 4 x Pro), 3.26 – 3.16 (m, 7H, Pro), 2.30 – 2.22 (m, 4H, 4 x Pro) 1.99 – 1.85 (m, 12H, 4 x Pro). Other peaks: 3.15 (s, MeOH). Chemical Formula: $[Zr_6O_4(OH)_4(TDC)_4(Pro)_4]$

Synthesis of DUT-67-trp: 40 mg (0.027 mmol) of DUT-67 were added in a 20 ml glass capped vial containing L-tryptophan (85 mg, 0.42 mmol) and 5 ml of EtOH. The resulting mixture was stirred at 80 ºC for 96 h. The white solid was washed with methanol (6 times), then dried at 60 ºC for 24 h. Yield: 46 mg. ^{1}H-NMR (Figure S6): δ 10.86 (s, Trp), 8.08 (s, 0.5H, 0.5 × HCOO), 7.70 (s, 8H, 4 x TDC), 7.52 (d, *J* = 7.9 Hz, 2H, 2 x Trp), 7.36 (d, *J* = 8.1 Hz, 2H, 2 x Trp), 7.19 (s, 2H, 2 x Trp), 7.09 (t, *J* = 7.6 Hz, 2H, 2 x Trp), 7.00 (t, *J* = 7.5 Hz, 2H, 2 x Trp), 3.25 (d, *J* = 6.1 Hz, 4H, 2 x Trp). Other peaks: 3.15 (s, MeOH). Acetone and DMF peaks also appear in the spectra due to impurities in the NMR tube. Formula: $[Zr_6O_4(OH)_{5.5}(TDC)_4(HCOO)_{0.5}(Trp)_2(solvent)_x]$

Table S1. Synthetic screening and parameter evaluation to obtain DUT-67-Pro and DUT-67-Trp.

Material	Solvent	Additive	Temperature (ºC)	Time (h)	Quantity of Amino-Acid per Zr_6O_8 node
DUT-67-Pro	DMF	-	25	120	-
DUT-67-Pro	DMF	HCl	25	120	1.3
DUT-67-Pro	DMF	HCl	80	48	1.7
DUT-67-Pro	EtOH	HCl	80	48	4.0
DUT-67-Trp[a]	EtOH	-	25	96	8.15
DUT-67-Trp[a]	EtOH	-	80	96	7.45
DUT-67-Trp[b]	EtOH	-	80	96	-
DUT-67-Trp[c]	EtOH	-	80	96	2

[a] Solid washed with EtOH, leading to Trp excess due to low solubility. [b] Solid washed with H_2O. [c] Solid washed with MeOH.

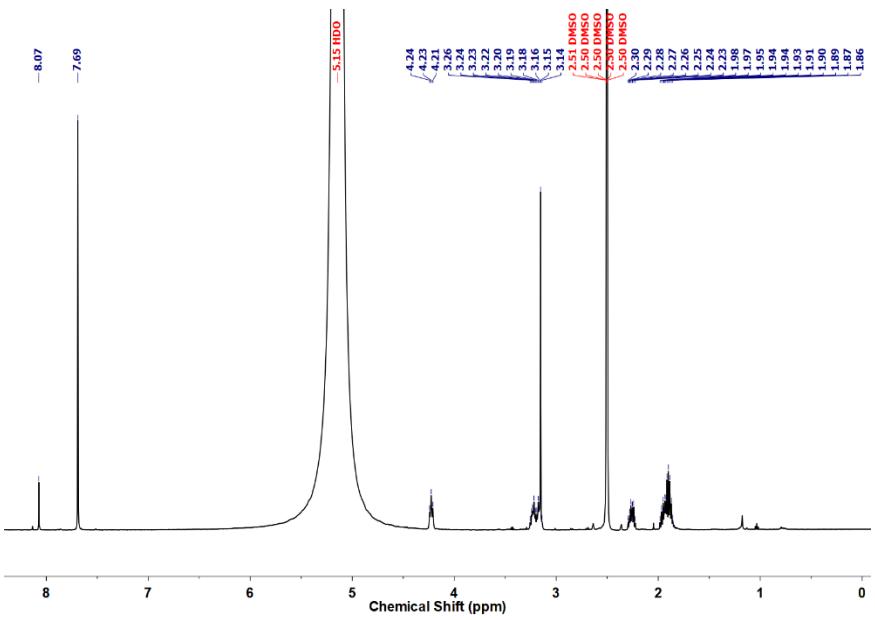

Figure S5. ^{1}H-NMR of DUT-67-Pro in DMSO-d_6:D_2O:HF (500 MHz).

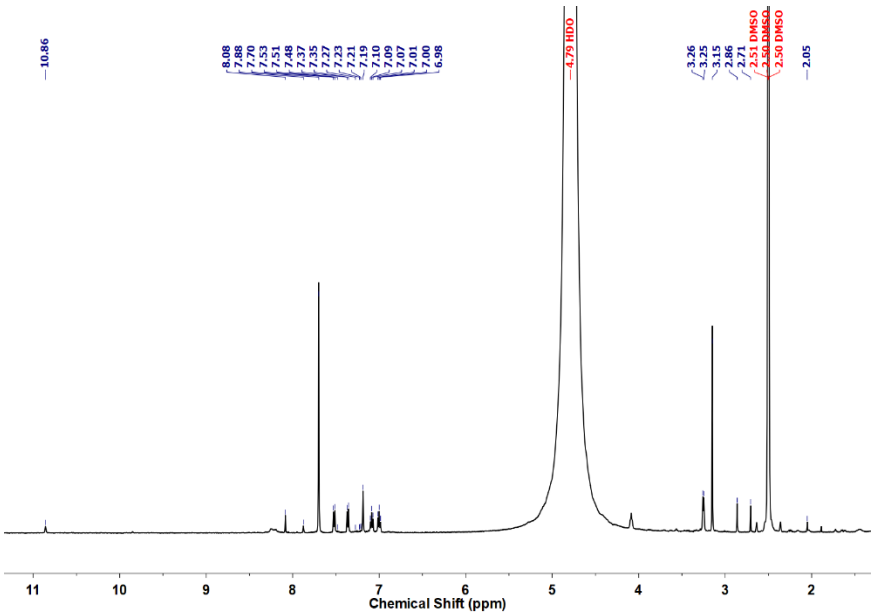

Figure S6. ^{1}H-NMR of DUT-67-Trp in DMSO-d_6:D_2O:HF (500 MHz).

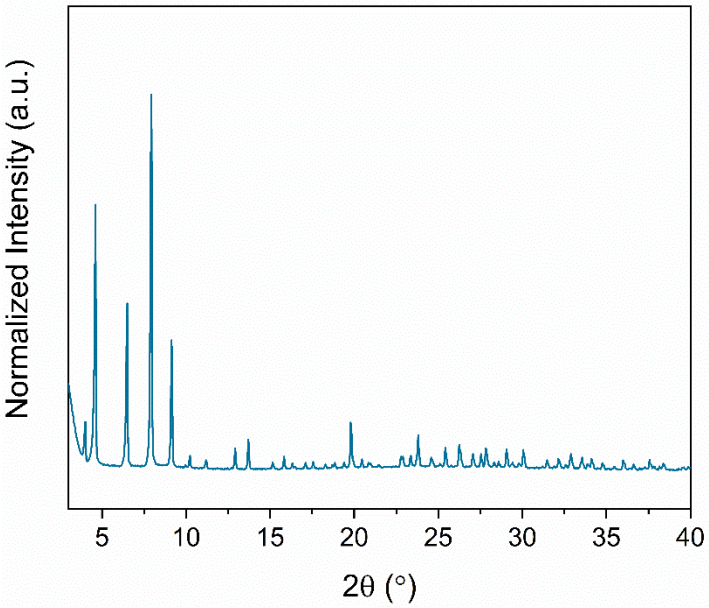

Figure S7. PXRD pattern of DUT-67-pro. No additional Bragg peaks are observed compared to the pattern of the pristine material. A change is seen in the intensity of Bragg peaks [2θ = 3.98°, (111) reflection, intensity increase // 2θ = 4.61°, (200) reflection, intensity decrease]. Both observations are in agreement with the introduction of large scattering material in the associated pore.[5]

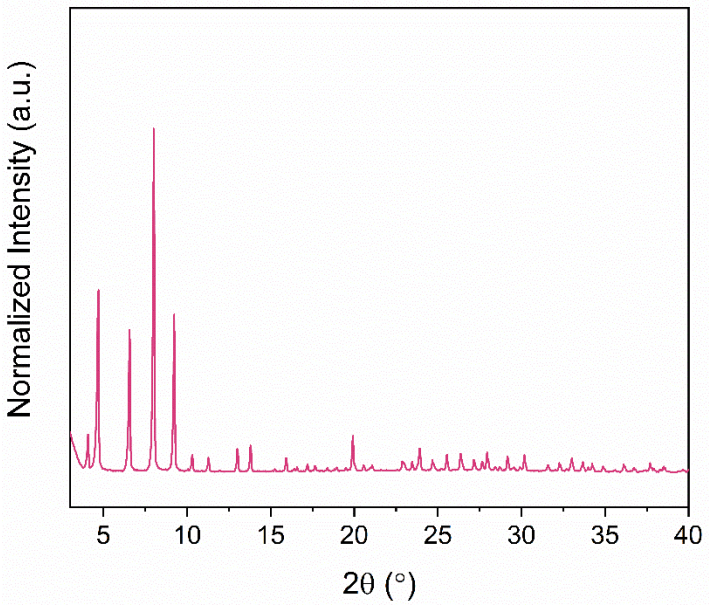

Figure S8. PXRD pattern of DUT-67-trp. Similar observations as in DUT-67-Pro are identified.

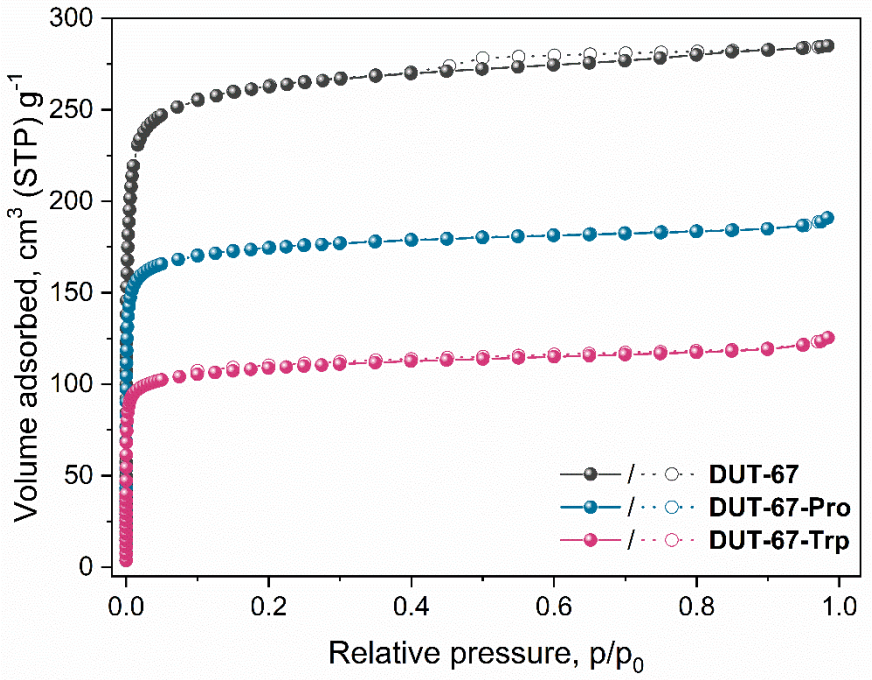

Figure S9. N_2 isotherms for all materials recorded at 77 K.

Table S2. Nitrogen uptake, pore volume (calculated at $p/p_0 = 0.99$) and BET surface area values materials of the MOFs of this study, as calculated from the N_2 isotherms.

Material	Uptake ($cm^3\ g^{-1}$)	Pore volume ($cm^3\ g^{-1}$)	BET surface area ($m^2\ g^{-1}$)
DUT-67	284.9	0.44	864
DUT-67-Pro	190.9	0.29	607
DUT-67-Trp	125.4	0.19	349

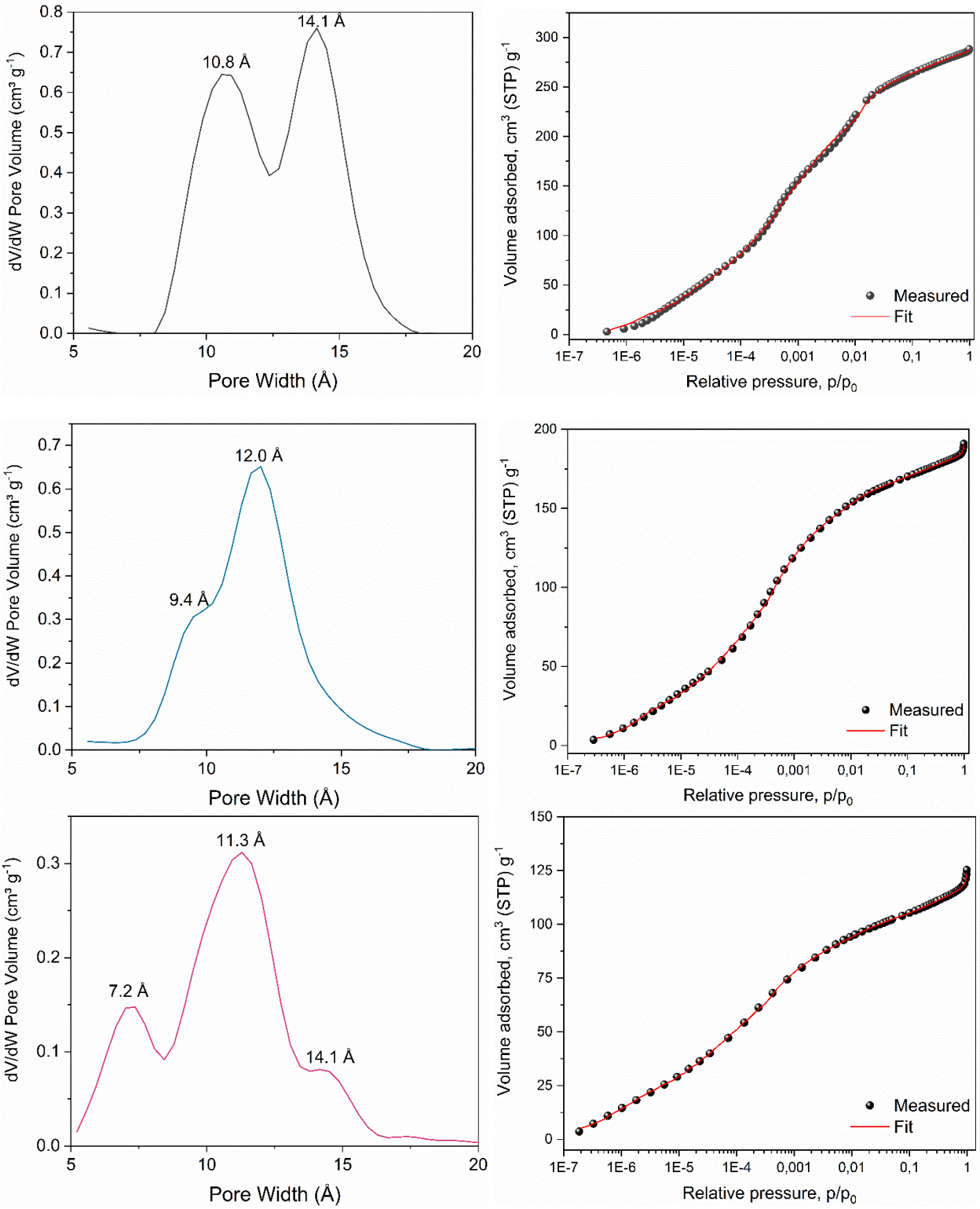

Figure S10. Pore size distribution (PSD) analysis (left) and corresponding NLDFT fits (right) for DUT-67 (top) DUT-67-Pro (middle), DUT-67-Trp (bottom) as calculated from the N_2 isotherms.

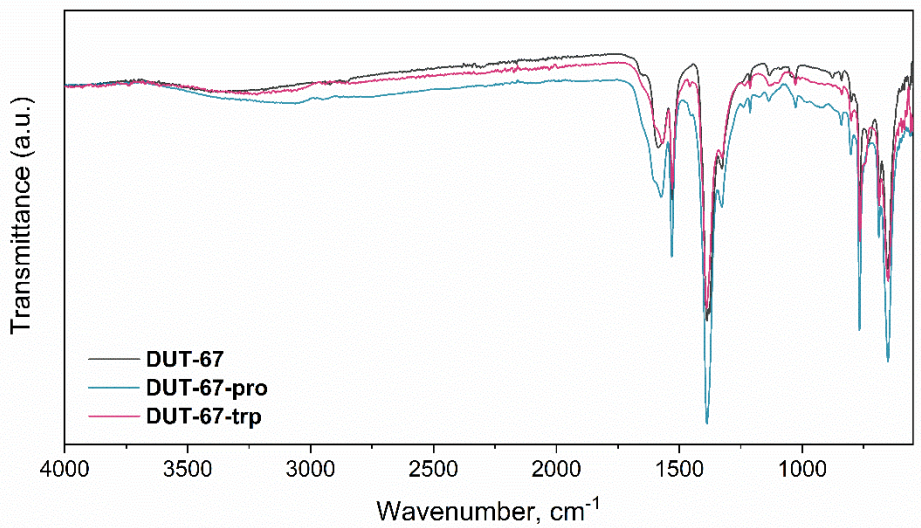

Figure S11. FT-IR spectra of all MOF materials of this study.

The FT-IR analysis shows very similar spectra for all relevant materials. In detail, all spectra display a strong peak at ~653 cm^{-1}, in excellent agreement to the existence of collective vibrations of Zr-O bonds within the Zr_6O_8 cluster node. Another strong peak appears at 765 cm^{-1} for all materials, corresponding to the vibration of C-S bonds in the thiophene-based TDC ligand. Other characteristic signals are observed at approximately 1575 and 1530 cm^{-1}, corresponding to the stretching of aromatic C=C bonds within the thiophene ring, and at the regions of 1390 and 1325 cm^{-1}, due to the asymmetric and symmetric vibrations of the carboxylate group. A broad signal also appears at the region of 3200-3400 cm^{-1} only in the spectra of the materials functionalized with amino-acids, and is associated to the stretching vibration of the N-H bond. Notably, these spectra show no signals related to the presence of uncoordinated –COOH groups, further confirming that the amino-acids coordinate to the inorganic node and are not found within the pores of the framework.

Supplementary Note 3. X-Ray Pair Distribution Function analysis

Synchrotron X-ray total scattering data suitable for pair distribution function (PDF) analysis were collected at the European Synchrotron Radiation Facility (ESRF), France (beamline ID15A, beamtime MA-5852) using 90 keV (0.13776 Å) X-rays. Samples were first ground into fine powder, then loaded into kapton capillaries (1.1 mm Ø) and sealed. Data scans were collected for 1 minute. Empty capillary and background total scattering data were corrected for in data

processing. Sample data were processed using PDFgetX3 to a Qmax of 22 $Å^{-1}$. Differential PDFs were obtained by subtraction of PDF profiles in real space after applying a normalization factor.

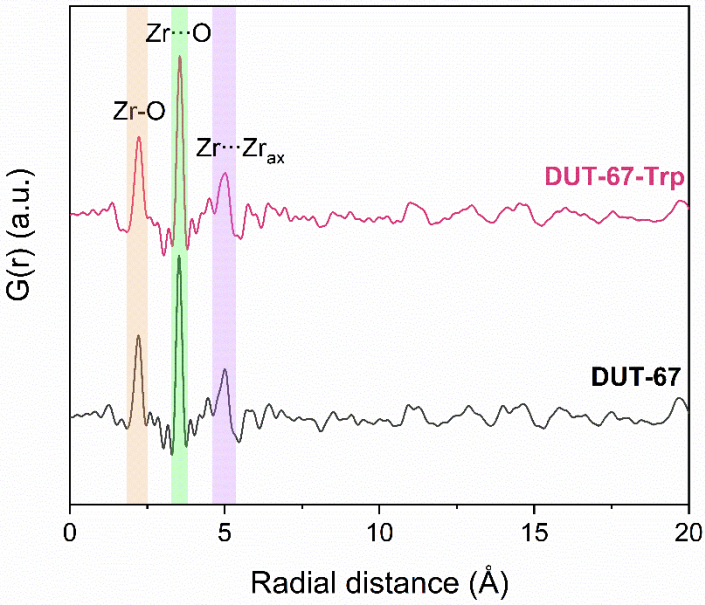

Figure S12. Total PDF data of DUT-67 and DUT-67-Trp.

Supplementary Note 4. Characterization of MOFs post-CO_2 sorption

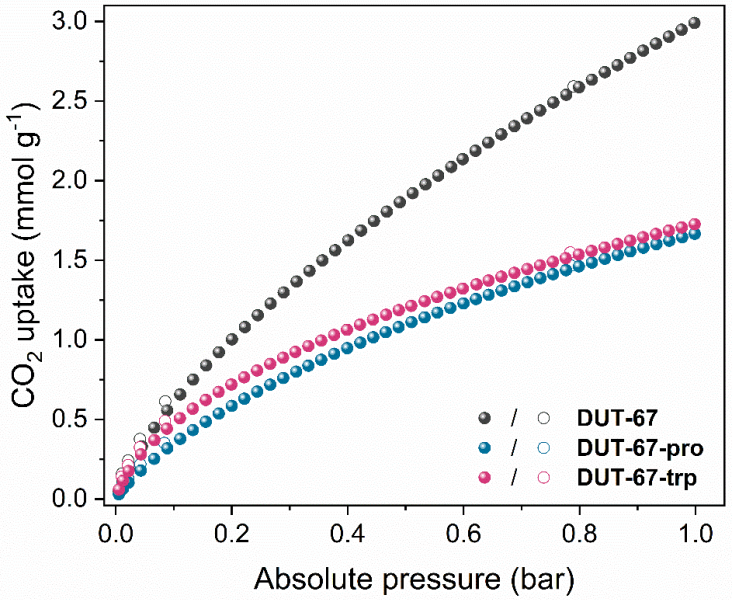

Figure S13. CO_2 isotherms for all materials of this study recorded at 273 K.

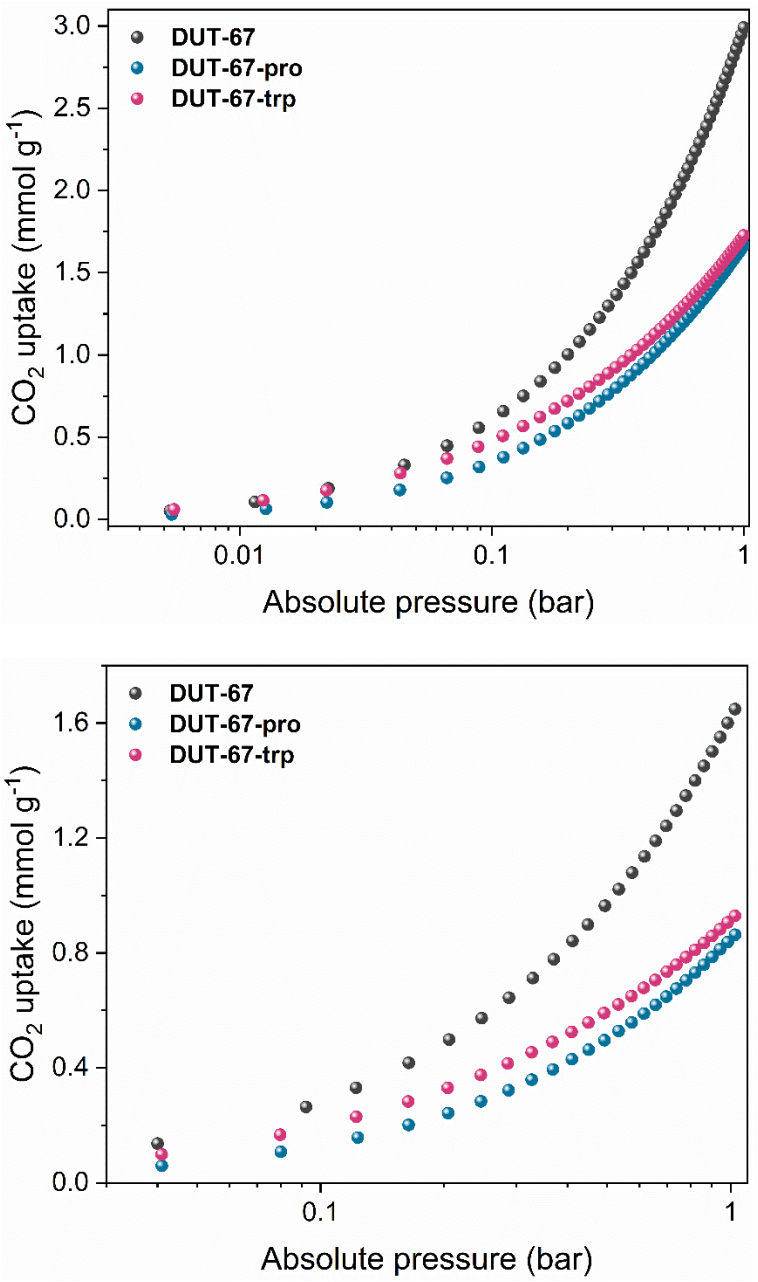

Figure S14. CO_2 isotherms in semi-logarithmic scale for all materials of this study recorded at 273 (top) and 298 (bottom) K.

Table S3. Numerical CO_2 isotherm data for pristine DUT-67 recorded at 273 K.

Adsorption			Desorption	
Absolute Pressure (bar)	Quantity Adsorbed (mmol/g)		Absolute Pressure (bar)	Quantity Adsorbed (mmol/g)
0.005287	0.051893		0.998242	2.98802
0.011504	0.105902		0.789981	2.58991
0.02247	0.188044		0.085425	0.612723
0.044992	0.330465		0.041655	0.376672
0.066416	0.447438		0.021351	0.24176
0.088767	0.556208		0.010689	0.15875
0.111048	0.656152			
0.133444	0.74966			
0.155926	0.838073			
0.178031	0.92113			
0.200507	1.00206			
0.222777	1.0793			
0.244904	1.15345			
0.267235	1.2262			
0.289512	1.29656			
0.311989	1.36551			
0.334164	1.43213			
0.356424	1.49743			
0.378698	1.56135			
0.40104	1.624			
0.423326	1.68532			
0.445286	1.74485			
0.467641	1.80418			
0.489925	1.86227			
0.512095	1.91908			
0.534421	1.97526			
0.556395	2.0298			
0.578776	2.08462			
0.598528	2.13303			
0.620602	2.18546			
0.642724	2.23706			
0.665036	2.28856			
0.687678	2.34011			
0.709456	2.38909			
0.731991	2.4391			
0.75467	2.48866			
0.777297	2.53762			
0.799228	2.58462			
0.821333	2.63159			
0.843739	2.67844			
0.865565	2.72349			
0.887481	2.76842			
0.909732	2.8135			
0.931973	2.85816			
0.954081	2.90201			
0.976187	2.94524			
0.998242	2.98802			

Table S4. Numerical CO_2 isotherm data for DUT-67-Pro recorded at 273 K.

Adsorption			Desorption	
Absolute Pressure (bar)	Quantity Adsorbed (mmol/g)		Absolute Pressure (bar)	Quantity Adsorbed (mmol/g)
0.005373	0.030482		0.99885	1.66427
0.01269	0.064218		0.785047	1.46577
0.022148	0.102773		0.083878	0.351722
0.043158	0.17856		0.042482	0.217882
0.066376	0.252426		0.020853	0.132977
0.089045	0.317844		0.010552	0.081659
0.111204	0.377386			
0.133195	0.432572			
0.155393	0.485272			
0.177793	0.536325			
0.20009	0.584815			
0.221819	0.629842			
0.244099	0.674309			
0.266551	0.717796			
0.288799	0.759337			
0.311341	0.799737			
0.33229	0.836569			
0.354374	0.874187			
0.376908	0.91096			
0.399257	0.946628			
0.422012	0.981876			
0.444291	1.01548			
0.465692	1.04712			
0.488177	1.07903			
0.510326	1.10987			
0.532622	1.14033			
0.554804	1.16975			
0.577306	1.19911			
0.599856	1.22785			
0.621401	1.25478			
0.643311	1.28171			
0.665542	1.30848			
0.687669	1.33511			
0.710314	1.36116			
0.732617	1.38635			
0.754343	1.41102			
0.776659	1.43578			
0.798967	1.46053			
0.821313	1.48458			
0.843805	1.50836			
0.866195	1.53174			
0.887684	1.55408			
0.910218	1.57703			
0.932642	1.59936			
0.954902	1.62132			
0.977105	1.64337			
0.99885	1.66427			

Table S5. Numerical CO_2 isotherm data for DUT-67-Trp recorded at 273 K.

Adsorption			Desorption	
Absolute Pressure (bar)	Quantity Adsorbed (mmol/g)		Absolute Pressure (bar)	Quantity Adsorbed (mmol/g)
0.005483	0.060742		0.998625	1.72519
0.012393	0.115415		0.784089	1.54761
0.022066	0.175954		0.084754	0.49017
0.043437	0.280381		0.041727	0.324065
0.066457	0.369375		0.021111	0.213024
0.088297	0.441615		0.010549	0.141487
0.110609	0.507134			
0.132934	0.56646			
0.155349	0.621437			
0.177546	0.671984			
0.199334	0.718797			
0.221548	0.764			
0.243799	0.806821			
0.266381	0.848385			
0.288695	0.887705			
0.30995	0.923913			
0.33216	0.960449			
0.354386	0.995179			
0.376712	1.02954			
0.398802	1.06209			
0.421269	1.09442			
0.443606	1.12612			
0.466244	1.1565			
0.488373	1.18568			
0.509776	1.21277			
0.532996	1.24188			
0.554257	1.26799			
0.577032	1.29517			
0.598806	1.32071			
0.622456	1.34763			
0.643136	1.37101			
0.665331	1.39518			
0.687723	1.41946			
0.709836	1.44315			
0.731772	1.46616			
0.753958	1.48907			
0.776271	1.51202			
0.79858	1.53458			
0.820895	1.5571			
0.843205	1.57933			
0.865633	1.60075			
0.887341	1.62193			
0.909662	1.64324			
0.93201	1.6638			
0.954302	1.6846			
0.976297	1.70489			
0.998625	1.72519			

Table S6. Numerical CO_2 isotherm data for pristine DUT-67 recorded at 298 K.

Adsorption			Desorption	
Absolute Pressure (bar)	Quantity Adsorbed (mmol/g)		Absolute Pressure (bar)	Quantity Adsorbed (mmol/g)
0.040031	0.13628		0.984025	1.63541
0.092188	0.263986		0.862263	1.50263
0.122013	0.330516		0.740244	1.36158
0.164091	0.41725		0.61757	1.20999
0.20595	0.497817		0.493639	1.04503
0.247133	0.572303		0.370477	0.865396
0.288338	0.643723		0.247783	0.664447
0.32947	0.711878		0.123743	0.423293
0.370435	0.777422		0.062168	0.27501
0.411675	0.841122		0.031339	0.188443
0.448551	0.897803			
0.493597	0.963557			
0.533624	1.0207			
0.575212	1.07857			
0.616716	1.13501			
0.656482	1.18864			
0.69625	1.2408			
0.737808	1.29445			
0.778218	1.34638			
0.819625	1.39885			
0.860414	1.44941			
0.90155	1.49988			
0.943203	1.55006			
0.983725	1.59896			
1.02476	1.64693			

Table S7. Numerical CO_2 isotherm data for DUT-67-Pro recorded at 298 K.

Adsorption			Desorption	
Absolute Pressure (bar)	Quantity Adsorbed (mmol/g)		Absolute Pressure (bar)	Quantity Adsorbed (mmol/g)
0.041013	0.059027		0.988339	0.871411
0.079995	0.107774		0.861422	0.801276
0.123223	0.157222		0.739648	0.728193
0.163978	0.200994		0.616786	0.646794
0.204652	0.242611		0.493079	0.555494
0.246238	0.283245		0.369778	0.45499
0.287438	0.321679		0.25282	0.347365
0.327423	0.35822		0.12341	0.210781
0.368692	0.394308		0.061726	0.133248
0.410154	0.429917		0.030949	0.088513
0.450773	0.462835			
0.492534	0.496053			
0.533578	0.527884			
0.573671	0.557674			
0.614955	0.588408			
0.656196	0.618539			
0.697126	0.647243			
0.737657	0.675305			
0.778747	0.703983			
0.819783	0.731215			
0.86093	0.758481			
0.90204	0.785028			
0.94293	0.812169			
0.98409	0.837268			
1.02565	0.862533			

Table S8. Numerical CO_2 isotherm data for DUT-67-Trp recorded at 298 K.

Adsorption			Desorption	
Absolute Pressure (bar)	Quantity Adsorbed (mmol/g)		Absolute Pressure (bar)	Quantity Adsorbed (mmol/g)
0.040988	0.09893		0.988031	0.942557
0.079753	0.167013		0.863549	0.885053
0.122197	0.229422		0.740275	0.821658
0.163591	0.282472		0.616571	0.749501
0.204247	0.330014		0.492866	0.666834
0.246017	0.374891		0.369872	0.570569
0.286153	0.414961		0.246779	0.455223
0.327224	0.45343		0.123678	0.305491
0.367816	0.489961		0.061969	0.201442
0.409443	0.524587		0.031154	0.132141
0.44994	0.557093			
0.491559	0.59006			
0.532502	0.62013			
0.573312	0.649342			
0.614191	0.677873			
0.655135	0.705207			
0.699336	0.734415			
0.737694	0.758643			
0.778917	0.784496			
0.81954	0.810059			
0.861029	0.833914			
0.901792	0.858336			
0.942481	0.882014			
0.98366	0.90538			
1.02506	0.928199			

Table S9. Maximum volumetric CO_2 uptake values for all materials of this study.

Material	**CO_2 uptake [cm^3 (STP)/g]**	
	273 K	**298 K**
DUT-67	67.0	36.9
DUT-67-Pro	37.3	19.3
DUT-67-Trp	38.7	20.8

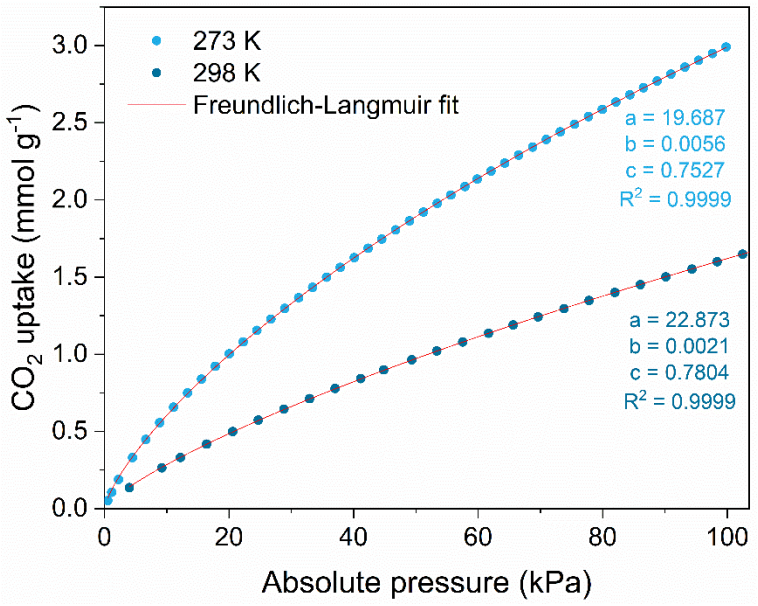

Figure S15. Freundlich-Langmuir fit for CO_2 isotherms of pristine DUT-67 at 273 and 298 K.

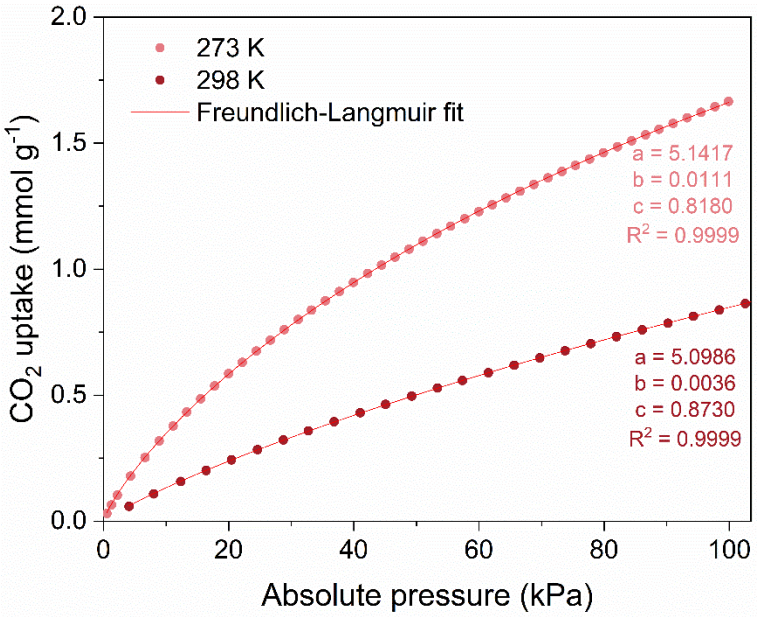

Figure S16. Freundlich-Langmuir fit for CO_2 isotherms of DUT-67-Pro at 273 and 298 K.

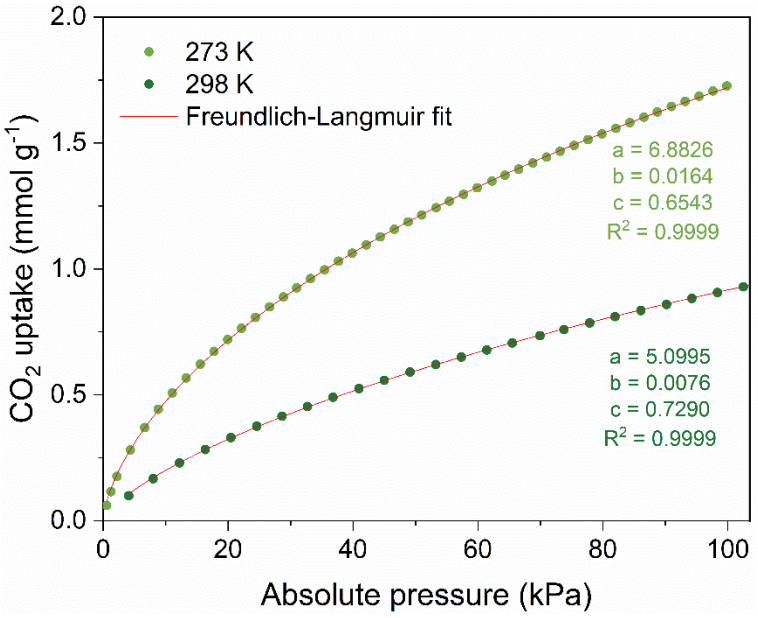

Figure S17. Freundlich-Langmuir fit for CO_2 isotherms of DUT-67-Trp at 273 and 298 K.

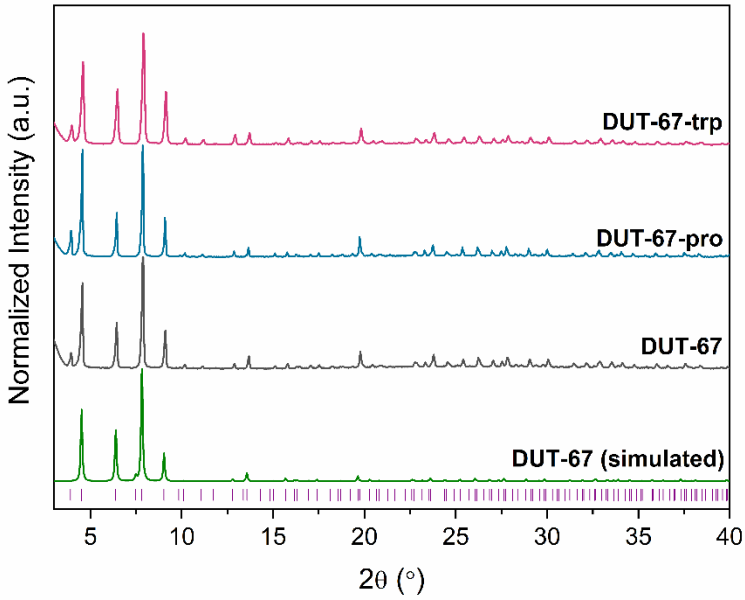

Figure S18. PXRD patterns of all materials of this study, after two CO_2 sorption cycles and subsequent activation. Purple lines denote the expected Bragg peaks as derived from the simulated PXRD pattern of DUT-67.

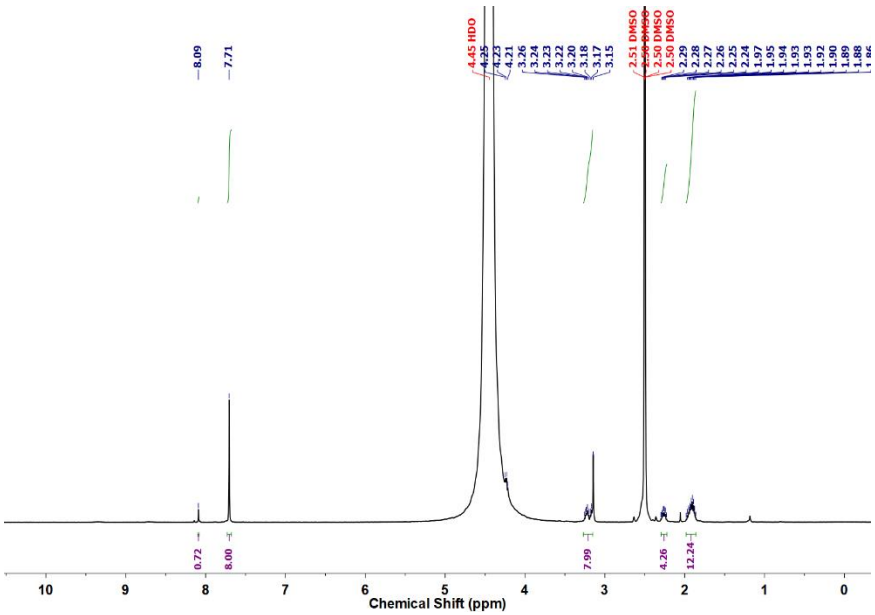

Figure S19. ^{1}H-NMR of DUT-67-Pro after two CO_2 sorption cycles and subsequent activation, in DMSO-d_6:D_2O:HF (500 MHz).

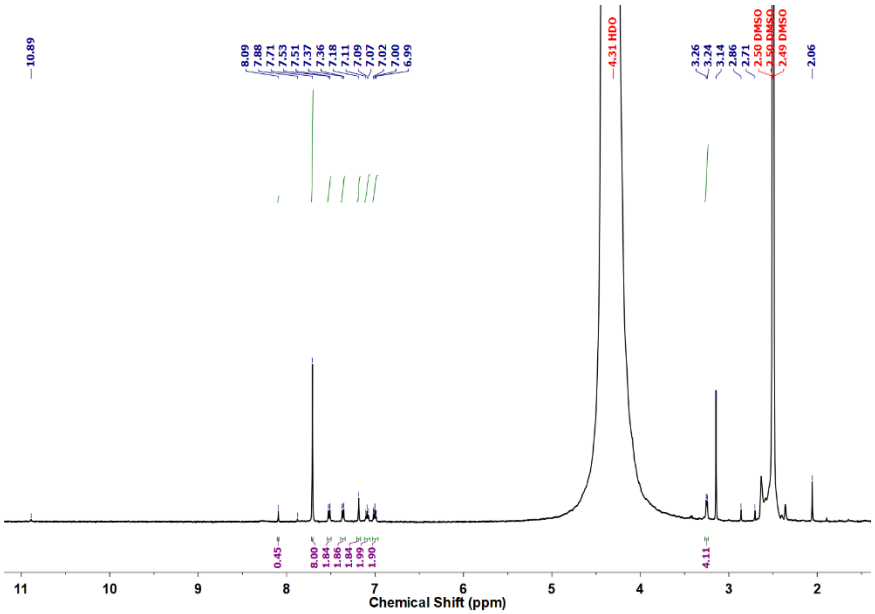

Figure S20. ^{1}H-NMR of DUT-67-Trp after two CO_2 sorption cycles and subsequent activation, in DMSO-d_6:D_2O:HF (500 MHz).

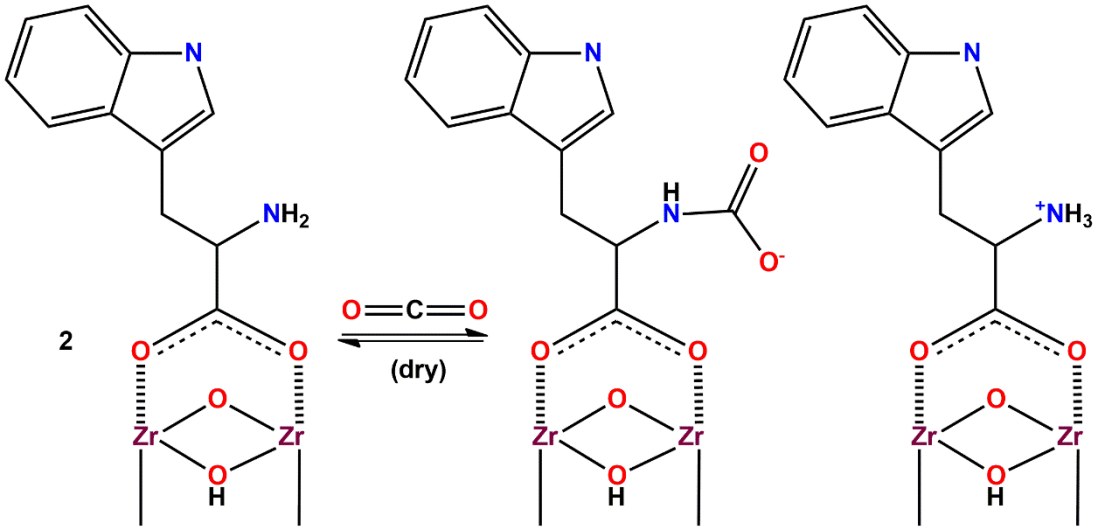

Figure S21. Proposed formation of the carbamate intermediate in DUT-67-Trp during CO_2 sorption[6-9].

Supplementary Note 5. Dynamic Breakthrough CO_2 analysis

Basic Activation of the materials. In order to increase the affinity of the adsorbents for CO_2 molecules and to implement capture, a basic activation process was carried out. For this purpose, 430 mg of DUT-67-Pro were suspended in 90 mL of a 0.016 M NaOH solution in methanol. For the activation of DUT-67-Trp, 487 mg were suspended in 100 mL of a 0.008M solution. After 30 minutes under stirring at room temperature, the materials were isolated and washed, and dried at 60 °C in the oven for 16 hours. The correct deprotonation of the amino groups was followed by measuring the acidity of a suspension of 3 mg of the material in 1 mL of water with a pH-meter. The values obtained were 5.77 for DUT-67-Pro and 4.88 for DUT-67-Trp, higher than those measured prior to activation, 3.36 and 3.63 respectively.

Dynamic Breakthrough Analysis. Dynamic breakthrough measurements were conducted to test the CO_2 adsorption efficiency of these materials, in the terms of practical direct air capture (DAC) applications[10]. This type of sorption experiment is imperative since most real-life adsorption processes involve high gas flow rates and the presence of water. DUT-67-Pro and DUT-67-Trp were studied for CO2 uptake under varying RH levels from 0 to 50% to investigate the relevance

of water vapor in the capture process. The samples were activated within the reaction column, at 140 ºC for 1 hour under N_2 continuous flow (20 mL/min). Then, the desired gas was feed (20 mL/min N_2, with 15% CO_2) at different humidity levels (0-50% RH). The different levels of humidity were controlled by adjusting the blend ratio of a water-saturated N_2 flow. The CO_2 uptake values were calculated by numerical integration of the breakthrough curves obtained experimentally.

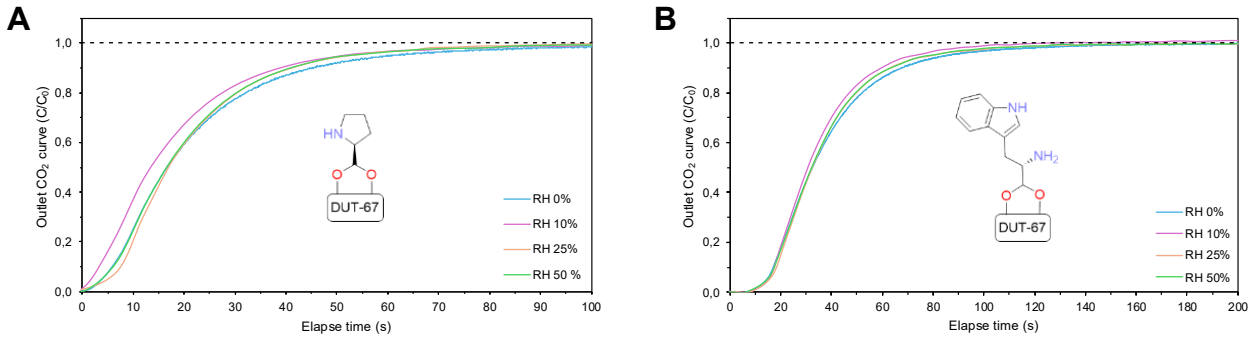

Figure S22. Dynamic CO_2 breakthrough curves of the materials: (A) DUT-67-Pro and (B) DUT-67-Trp**.**

For either DUT-67-Pro or DUT-67-Trp, the results under dry conditions (0.248 and 0.271 mmol g^{-1}) show large decreases in CO_2 uptake compared to the respective single component CO_2 isotherms. This behaviour can be associated to the short contact time between the adsorbate and the adsorbent coupled with the slow kinetics of the interaction between the material and CO_2, which was also observed during isotherm measurements. Also, this value could be related to the softer activation conditions used compared with the ones applied for single component CO_2 isotherms. As detailed in the main text, the behaviour of each material shows considerable changes as the level of relative humidity increases: In DUT-67-Pro, introduction of 10 and 25% RH decreases the uptake down to 0.171 mmol g^{-1}, while a moisture level of up to 50% RH brings the uptake down to 0.133 mmol g^{-1}. In the case of DUT-67-Trp, a significant rise in adsorption capacity is observed after increasing the relative humidity up to 25% or 50%, with the material reaching an adsorption capacity of 0.281 mmol g^{-1}.

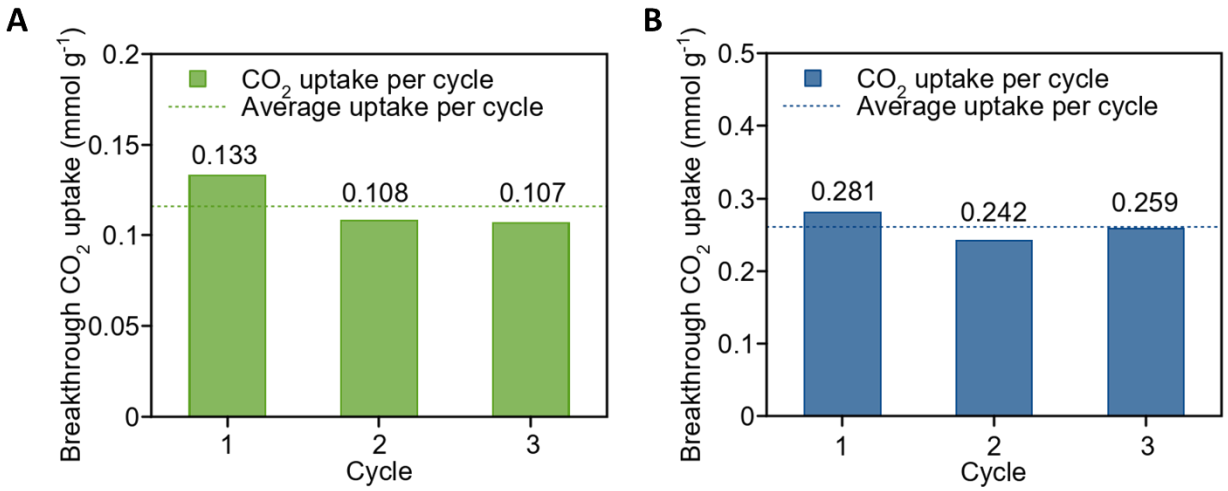

Figure S23. CO_2 uptakes of **(A)** DUT-67-Pro and **(B)** DUT-67-Pro at 50% RH (15% CO_2, 85% N_2 at 298 K).

Supplementary References

1 E. Loukopoulos, S. Marugán-Benito, D. Raptis, E. Tylianakis, G. E. Froudakis, A. Mavrandonakis and A. E. Platero-Prats, *Advanced Functional Materials*, 2024, **34**, 2409932.

2 C. F. Macrae, P. R. Edgington, P. McCabe, E. Pidcock, G. P. Shields, R. Taylor, M. Towler and J. van De Streek, *J. Appl. Crystallogr.*, 2006, **39**, 453-457.

3 A. Nuhnen and C. Janiak, *Dalton Transactions*, 2020, **49**, 10295-10307.

4 K. D. Nguyen, C. Kutzscher, F. Drache, I. Senkovska and S. Kaskel, *Inorganic Chemistry*, 2018, **57**, 1483-1489.

5 R. Li, S. Alomari, R. Stanton, M. C. Wasson, T. Islamoglu, O. K. Farha, T. M. Holsen, S. M. Thagard, D. J. Trivedi and M. Wriedt, *Chem Mater*, 2021, **33**, 3276-3285.

6 M. Gupta and H. F. Svendsen, *Journal of Physical Chemistry B*, 2019, **123**, 8433-8447.

7 H. Lyu, O. I. F. Chen, N. Hanikel, M. I. Hossain, R. W. Flaig, X. Pei, A. Amin, M. D. Doherty, R. K. Impastato, T. G. Glover, D. R. Moore and O. M. Yaghi, *Journal of the American Chemical Society*, 2022, **144**, 2387-2396.

8 T. M. McDonald, J. A. Mason, X. Kong, E. D. Bloch, D. Gygi, A. Dani, V. Crocellà, F. Giordanino, S. O. Odoh, W. S. Drisdell, B. Vlaisavljevich, A. L. Dzubak, R. Poloni, S. K. Schnell, N. Planas, K. Lee, T. Pascal, L. F. Wan, D. Prendergast, J. B. Neaton, B. Smit, J. B. Kortright, L. Gagliardi, S. Bordiga, J. A. Reimer and J. R. Long, *Nature*, 2015, **519**, 303-308.

9 R. B. Said, J. M. Kolle, K. Essalah, B. Tangour and A. Sayari, *ACS Omega*, 2020, **5**, 26125-26133.

10 O. I. Chen, C. H. Liu, K. Wang, E. Borrego-Marin, H. Li, A. H. Alawadhi, J. A. R. Navarro and O. M. Yaghi, *Journal of the American Chemical Society*, 2024, **146**, 2835-2844.